Generic Simulation Model for DFIG and Full Size Converter based Wind Turbines

Jens Fortmann, Stephan Engelhardt, Jörg Kretschmann, Christian Feltes, Martin Janßen, Tobias Neumann, Istvan Erlich

***Abstract*-- There is an increased international interest in electrical simulation models of wind turbines for stability analysis and interconnection studies. So-called "generic" models, with a model structure that is publicly available, have been required in the USA by many utilities. A working group of the Western Electricity Coordinating Council (WECC) and IEEE has developed models for different types of generators, among others for wind turbines using doubly fed induction generators (DFIG) and full size converters (FSC). Those models were so far mainly used in the USA, and the models were able to represent wind turbines with respect to common US grid code requirements.**

Due to an increased international interest in generic models, there is a need for updating existing models in order to (1) improve the representation of specific grid code requirements like reactive power contribution during grid faults, (2) to take into account ongoing technological developments (especially of DFIG) and (3) to improve the accuracy of the model since validation requirements in many countries now require a comparison with measurements.

The generic generator model presented in this paper allows an improvement of existing WECC/IEEE type 3 (DFIG) and type 4 (FSC) models especially during grid faults and during voltage recovery. The model is designed to represent both modern DFIG and different types of full size converter wind turbines.

The results of simulations using the proposed generator model are compared to measurements of voltage dips.

The new generic generator model will be proposed as extension for the WECC/IEEE generator models as well as basis for the draft of the IEC TC88 working group 27 (61400-27) on modeling and model validation.

***Index Terms*—Wind Energy, Standards, Measurement, Control**

I. Introduction

Generic simulation models for wind turbines based on an disclosed model structure gain increasing international acceptance. A set of models for different wind turbine types has been developed by a working group of the Western Electricity Coordinating Council (WECC), the further development is now coordinated within IEEE.

A generator model for DFIG and FSC based wind turbines has been proposed by WECC [1], (DFIG is described as "type 3" by WECC, FSC as "type 4'). Simulation results of the DFIG were compared to simulations with a more detailed model in [2]. Those models were so far mainly used in the USA, and the models were able to represent wind turbines with respect to common US grid code requirements.

One goal of generic models is to keep the handling simple by simplifying the model structure and reducing the number of parameters required. This inevitably leads to the some loss of some accuracy. One of the key tasks is therefore to find a good balance between model accuracy and model complexity.

European grid code requirements often have specific requirements on reactive power delivery during and following grid faults [3][4][5]. New regulations in Germany [6],[7] and Spain [8] require the validation of wind turbine simulation models with measurements of voltage dips.

An evaluation of the existing WECC type 3 generator models showed that it lacks the capability to control reactive power during grid faults. Other reduced order models that allow a very good representation of the DFIG [9] are very complex. Therefore, a new generic generator model is needed that offers both a satisfying accuracy during grid faults and a relatively simple modeling approach.

The comparison of simulations and measurements of modern DFIG and FSC based wind turbines shows that there are only limited differences between both technologies with respect to active and reactive currents during and following grid faults. Therefore, a modular approach has been chosen that allows the model to be used both for DFIG and FSC model simulation using different parameters.

II. Model of the DFIG

The DFIG is the most commonly used device for wind power generation. As is generally known, the rotor terminals are fed with a symmetrical three-phase voltage of variable frequency and amplitude. This voltage is provided by a voltage source converter usually equipped with IGBT based power electronics circuitry. The basic structure is shown in Fig. 1.

J. Fortmann is with REpower Systems AG, 24783 Osterrönfeld, Germany (e-mail: j.fortmann@repower.de);
S. Engelhardt is with Woodward SEG, 47906 Kempen, Germany (e-mail: stephan.engelhardt@woodward.com);
J. Kretschmann is with Woodward SEG, 47906 Kempen, Germany (e-mail: joerg.kretschmann@woodward.com);
C. Feltes is with the University Duisburg-Essen, 47057 Duisburg, Germany (e-mail: christian.feltes@uni-due.de)
M. Janßen is with Converteam GmbH, Culemeyerstr. 1,12277 Berlin,
T. Neumann is with the University Duisburg-Essen, 47057 Duisburg, Germany, (e-mail: tobias.neumann@uni-due.de)
I. Erlich is with the University Duisburg-Essen, 47057 Duisburg, Germany (e-mail: istvan.erlich@uni-due.de)

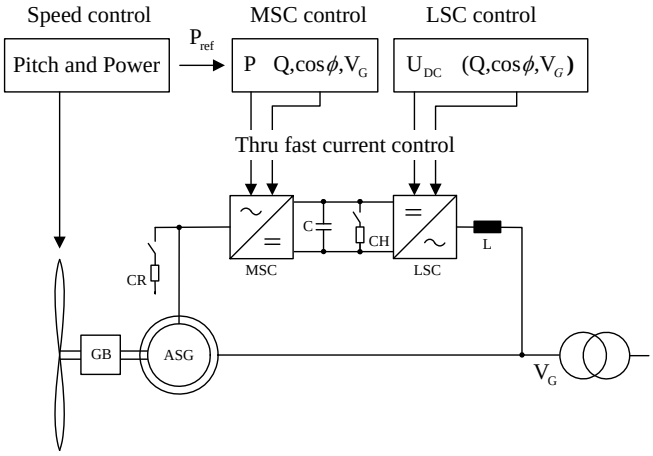

Fig. 1. Key components of DFIG system

A. Limitations of older DFIG designs

In older DFIG designs, protection against over-currents and undesirably high DC voltage was provided by the crowbar (CR) placed on the rotor side of the machine side converter (MSC). Very high rotor current following voltage dips could cause the DC voltage to exceeded the upper threshold allowed. The CB thyristor switches were then activated and the rotor terminals short-circuited through the CB resistance.

As a result, the DFIG then operated as a conventional slip-ring induction machine without any control capability left for the MSC and the line side converter (LSC).

An improved design allowed for faster control of the DC - link voltage, so at least the LSC could remain in operation while the crowbar was active and compensate some of the reactive power requirements of the generator during the fault.

IGBT-based crowbar designs of some manufacturers allowed for a shorter activation time of the crowbar, thereby reducing the time the MSC had to be deactivated.

All these designs are highly nonlinear and usually require detailed EMT - models to exactly represent the DC-currents that lead to the triggering of the crowbar. In [10] a model approach was presented that allowed a detailed simulation even with RMS models. Still, a rather detailed model is needed.

B. Improved protection of modern DFIG

New DFIG designs use a higher rating of the MSC and passive or active DC-link elements. One common approach is using an IGBT switched resistor connected to the DC-link, referred to as “chopper” that limits the voltage in case the currents fed into the DC-link are higher than the currents the LSC can feed into the grid. As a result, an activation of the crowbar following grid faults is not necessary any more and MSC and LSC remain controllable during the whole fault period.

C. DFIG model representations

The DFIG voltage and flux equations yield

$$\underline{v}_S = r_S \underline{i}_S + \frac{d\underline{\psi}_S}{dt} + j\omega_0 \underline{\psi}_S \tag{1}$$

$$\underline{v}_R = r_R \underline{i}_R + \frac{d\underline{\psi}_R}{dt} + j\left(\omega_0 - \omega_R\right)\underline{\psi}_R \tag{2}$$

$$\underline{\psi}_S = l_S \underline{i}_S + l_h \underline{i}_R \tag{3}$$

$$\underline{\psi}_R = l_h \underline{i}_S + l_R \underline{i}_R \tag{4}$$

with $l_S = l_h + l_{\sigma S}$ and $l_R = l_h + l_{\sigma R}$

The reduced order model (ROM) described in [10] for the positive sequence system is derived by setting the stator flux derivate to zero

$$\frac{d\underline{\psi}_S}{dt} = 0 \tag{5}$$

Then for Eq. (1) can be written after some algebraic manipulation and by using (3) and (4)

$$\underline{v}_S = \underline{z}' \underline{i}_S + \underline{v}_1' \tag{6}$$

The internal transient impedance can be written as

$$\underline{z}' = r_S + j\omega_0 l' \tag{7}$$

with

$$l' = l_s - \frac{l_h^2}{l_R} \quad (8) \qquad \text{and} \qquad k_R = \frac{l_h}{l_R} \tag{9}$$

and

$$\underline{v}_1' = j\omega_0 \frac{l_h}{l_R} \underline{\psi}_R = j\omega_0 k_R \underline{\psi}_R \tag{10}$$

as the corresponding transient driving Thévenin voltage source. Fig. 2 shows the corresponding Thévenin and Norton equivalents of the reduced order DFIG model.

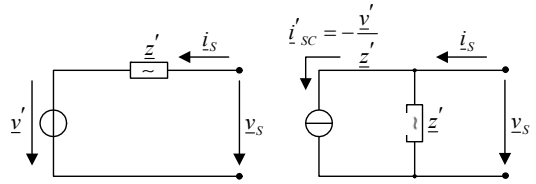

Fig. 2. Thévenin and Norton equivalent for coupling with the grid

D. Block diagram representation of DFIG

Replacing $\underline{i}_R$ in (2) with (4) yields the differential equation for the rotor flux in (11)

$$\frac{d\underline{\psi}_R}{dt} = -\frac{r_R}{l_R}\underline{\psi}_R - j\left(\omega_0 - \omega_R\right)\underline{\psi}_R + k_R r_R \underline{i}_S + v_R \tag{11}$$

Equation (11) describes the dynamic change of the rotor flux which forms the Thévenin resp. Norton source shown in Fig. 2. The model (11) including the Norton equivalent can also be described in the form of a block diagram shown in Fig. 3

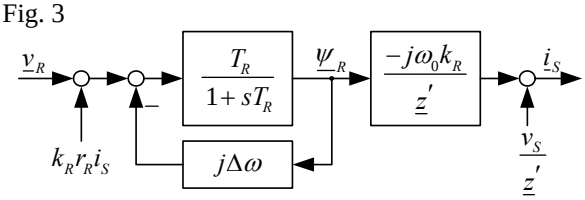

Fig. 3. Block diagram of machine equations

The following substitutions are introduced:

$$T_R = \frac{l_R}{r_R} \quad (12) \qquad \text{and} \qquad \Delta\omega = \left(\omega_0 - \omega_R\right) \quad (13)$$

A detailed description of the MSC control design is been given in [10]. Using a representation with complex variables, the rotor control loop is presented in Fig. 4:

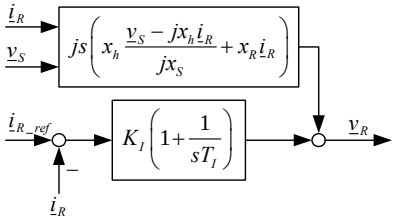

Fig. 4. Rotor Current Control

By aggregating the machine model of Fig. 3 and the control model of Fig. 4 we come up with the detailed structure presented in Fig. 5 for the entire model of DFIG control and machine.

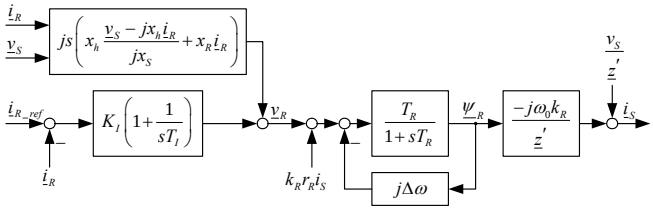

Fig. 5. Detailed model of machine and rotor current control

Based on this description, an aggregated model of DFIG control and machine in Fig. 6 can be deduced with

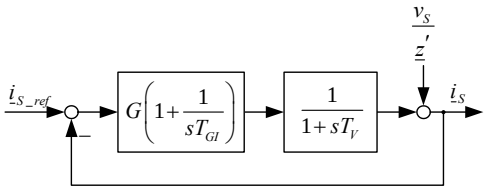

Fig. 6. Aggregated model of machine and rotor current control

the following simplifications:

- the coupling of the rotor flux components through $j\Delta\omega$ is neglected
- the cross coupling terms in control are not considered

Furthermore, the following aggregations are assumed:

- the rotor current is replaced by the stator current. that means the magnetizing current is not considered explicitly
- the feedback of stator current on rotor flux and the rotor current control are modeled by a single PI stator current controller
- the grid side converter is not considered separately but the effect is taken into account

As a consequence of this approach, the direct calculation of the parameters of the simplified model is not possible any more. An identification based on results of detailed simulation or measurements is necessary (see Fig. 7). By comparing the simulation results of the simplified models and using a heuristic optimization, the error of the model can be minimized. At the end of the iteration one gets the identified parameters for the model.

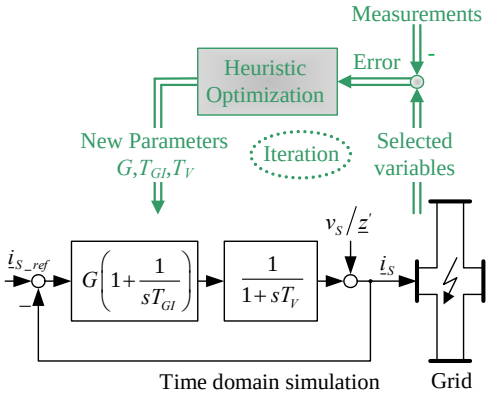

Fig. 7. Parameter Identification Procedure

III. Model of the FSC

The FSC has been used in wind turbines for more than two decades. A wide variety of generators exist at the moment, using synchronous wound rotors, permanent magnet synchronous machines or asynchronous machines, with gearbox, with a higher number of poles an a reduced gearbox and without gearbox. A typical structure is shown in Fig. 8. But from a grid connection point of view, the selection of the generator and the machine side converter does not influence the behavior towards the grid if MSC and LSC are decoupled by a DC link as it is usually the case in modern wind turbine designs. The generator and MSC are therefore represented as controllable current source only.

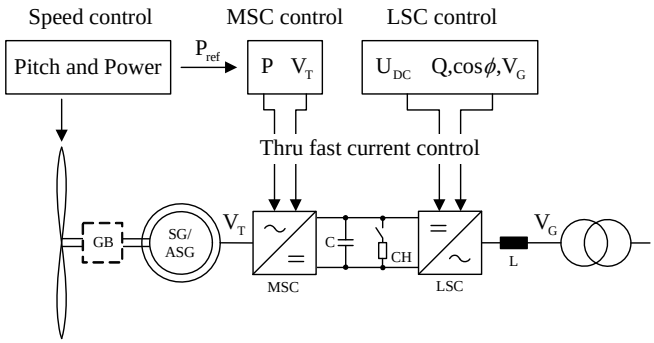

Fig. 8. Key components of FSC system

A. FSC model representation

As an approximation, the FSC can be seen as a fast acting voltage source (Thévenin equivalent) with a small delay described as first order lag. The impedance $\underline{z}$ (corresponding with the transient impedance $\underline{z}'$ of DFIG based system) can be defined as

$$\underline{z} = \underline{z}_C + \underline{z}_{Tr} \quad (14)$$

with

$\underline{z}_C$ = converter choke impedance

$\underline{z}_{Tr}$ = transformer impedance

Using a Norton equivalent for describing the FSC (see

Fig. 9), the current source is described by

$$\underline{i}'_{SC} = -\frac{\underline{v}_C}{\underline{z}} \tag{15}$$

with

$\underline{v}_C$: Voltage injected by the converter

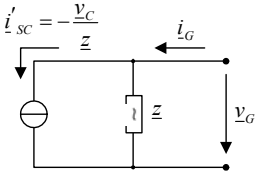

Fig. 9 Norton source representation

The structure of the FSC model using a simple PI-control for the LSC [8] with its components controller, converter and Norton source is shown in Fig. 10.

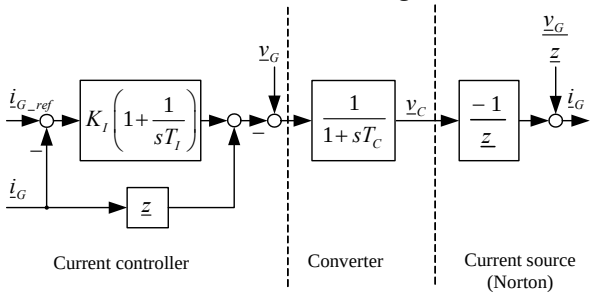

Fig. 10. Block diagram of current controller, converter and Norton source

By moving the impedance $\underline{z}$ from the Norton source into the controller, we obtain the following slightly modified structure (see Fig. 11)

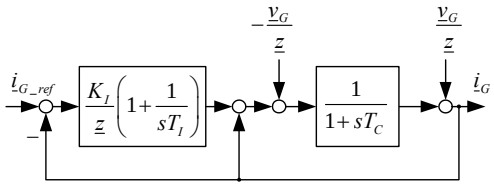

Fig. 11. Modified block diagram of current controller, converter and Norton source

The structure shown above can be approximated as follows with new values for the gain K_I and the time constant T_I

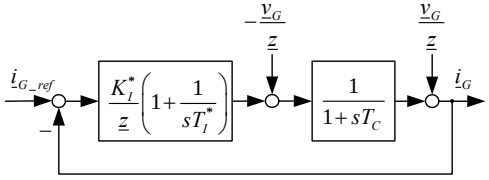

Fig. 12. Approximated model structure of FSC

The time constant T_C represents the delay of the converter which is very fast. Due to this fact the model can be further simplified as shown in Fig. 13.

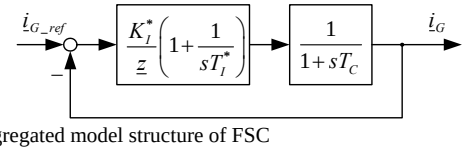

Fig. 13. Aggregated model structure of FSC

This representation corresponds with the generic model developed for DFIG wind turbines with the assumption of an infinite impedance $\underline{z}'$ (see Fig. 6).

IV. Model Structure

The model aggregation for the DFIG in Fig. 6 represents an aggregated model for generator and converter hardware and control. The model aggregation for the FSC in Fig. 13 represents the equivalent model for the converter hardware and control, the generator itself is represented as a controllable current source only.

The block diagram in Fig. 14 shows an implementation of the generator models using active and reactive current and turbine voltage as input and real and imaginary parts of the current (in grid coordinates) as output. Note that the PI-loop of the model is operating in grid coordinates and the transient impedance is considered by the transient reactance only.

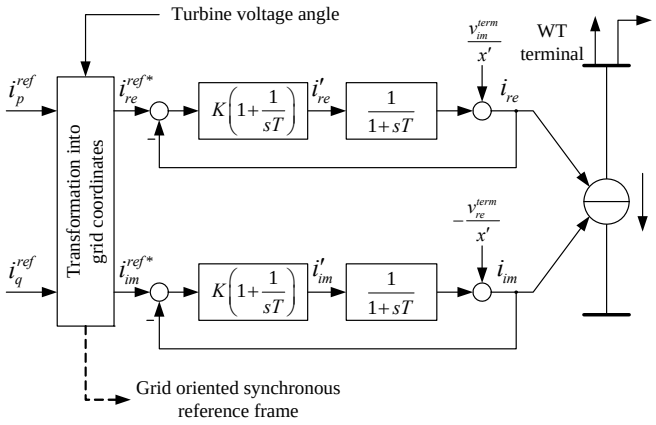

Fig. 14. Core of aggregated generator model of machine and current control as block diagram including terminals

This is a representation of the core functions, but key elements for a practical implementation have to be added. Wind turbine control offers a large number of control capabilities to limit active or reactive power output. In this proposal, it is assumed that the generator model contains functions common to all generator (and converter) systems. Functions that represent specific, possibly manufacturer specific functions are assumed to be part of a separate electrical control block. That block should contain the reference calculation for active and reactive currents.

This approach does not exactly represent the configuration in real turbines where functionality may be implemented either in the wind plant control, the turbine control or the converter. But it allows for a modular model design. Typical functions part of the electrical control block would be the calculation of the active current reference as function of external power reference, rotor speed and frequency and reactive current reference calculation as function of power factor, reactive power or voltage.

A. Current Limitation

The output current limitation of the generator model is

described in the current limitation block in Fig. 15.

(1) physical limits

(2) control limits

(3) dynamic limits

Short term thermal current limitations define physical limits for the maximum current the system can feed into the grid. These current limits of the DFIG and FSC are always defined by the converter that has far shorter time constants than the generator. Commonly, an active current priority is used during steady state operation while a reactive current priority may be used during very low or high voltage conditions. Depending on priority setting therefore the maximum allowed active or reactive current can be defined by (15).

$$i_{p\_\max} = \sqrt{i_{\max}^2 - i_q^2} \quad \text{or} \quad i_{q\_\max} = \sqrt{i_{\max}^2 - i_p^2} \tag{16}$$

Active and reactive current output may be further limited as function of the voltage. Although the actual implementation may be different, a good approximation can usually be achieved by defining a table that limits active and reactive current as function of voltage. In the case of active current limitations, the main reasons would be (a) reactive current priority during grid faults, (b) active current limitation to fulfill specific grid codes (c) active power limitation outside the standard voltage operating range and (d) grid stability limits at weak grid connection points [11]. Reasons for reactive current limitations as function of voltage are mainly (a) limiting the reactive power during normal operation (active power priority), (b) allow for increased reactive currents only during grid faults.

$$i_{p\_\max} = f(|u|) \quad \text{and} \quad i_{q\_\max} = f(|u|) \tag{17}$$

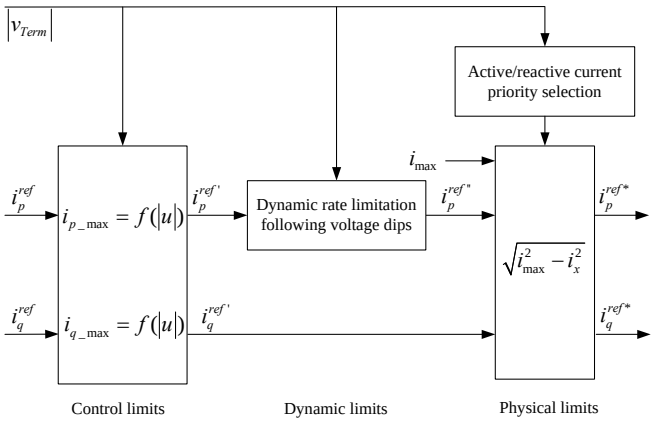

Fig. 15. Current limitation block

Dynamic control limits are needed to allow for an improved representation of active power recovery after grid faults. General ramp rate limitations are already implemented through the PT1 - block in Fig. 14. After grid faults, a slower recovery of active power may be implemented. Common reasons are (a) limiting shaft and gearbox loads (b) limiting DC-link voltage variations due to very fast active power changes. Depending on the manufacturer this function may be implemented as first order lag or as linear rate ramp limitation. Therefore a model should preferably allow for both methods.

In addition, there may be a delay after the voltage starts rising again until the active power increases. This can be due to control delays in the converter, a settling time needed by the PLL to synchronize again after voltage dips to very low voltages and as result of phase angle jumps after fault clearance. Generally, this delay is more relevant for very deep voltage dips.

The first order lag in Fig. 16 allows for a voltage dip dependant time delay. The recovery time can be varied by changing the time T, the delay until recovery by changing gain k. The rate limiter offers an additional parameter if a faster linear ramp rate is implemented.

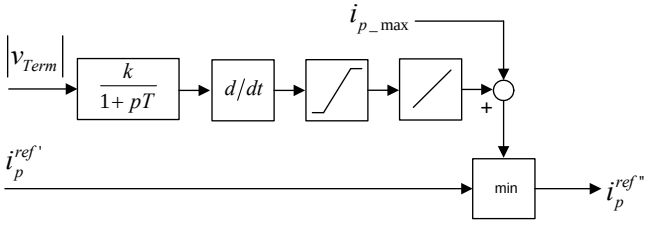

Fig. 16. Dynamic limitation block for defining a voltage dip dependant delay and ramp rate control after voltage dips.

B. Wind turbine transformer

The objective of a generic model representation is to achieve a reasonable approximation of reality using a simplified model structure. Currently different topologies exist on the market, controlling active an reactive power either on the gird side or on the turbine side of the transformer. If active power only is considered, the representation of a transformer would not be necessary. Also in the case of control on the grid side of a transformer, (up to date all commercial turbine connecting to the MV system have either a built-in or an external transformer) a transformer does not have to be modeled. But in the case active and reactive power are controlled on the turbine side of a transformer, it does have considerable impact to the reactive output both under normal operation conditions, but especially during grid faults. One reason is that in this case the current limitations are implemented on the low voltage side, so the maximum reactive power that can be achieved on the medium voltage side depends on the active power.

One possibility would be to add a separate transformer model in the case of turbine side control. But this would make it far more difficult to use this generator model as part of an aggregated wind plant. The transformer has impact both on the magnitude of the voltage as on the phase angle (18).

$$\underline{u}_2 = \underline{u}_1 - (r_{Tr} + jx_{Tr})\underline{i}_1 \tag{18}$$

By adding an equation with two parameters (18), a simple transformer model allows to include the transformer in the case of low voltage control or - by setting the two parameters to zero, to take out the transformer in the simulation model.

C. DC-link energy absorber for FSC

In the case of grid faults, the energy that can be trans-

ferred into the grid is limited both for physical reasons as due to the limited current capability of converters. Since the energy provided by the wind does not change necessarily, a grid fault with voltages below 90% rated voltage at rated power will lead to an increase of the rotor speed. By changing the blade pitch angle, the power input form the wind can be reduced, but the time constants of the pitch system are long compared to the duration of grid faults. Unless additional measures are taken, a turbine with FSC reacts comparable to a turbine with DFIG.

Some FSC technologies use an additional device to absorb the energy provided by the generator in the case of grid faults. A common implementation is a controllable resistor in the DC-link that absorbs the energy that can not be transferred to the grid in the case of grid faults. As a result the mechanical power p_{mech} and the electrical power p_{el} are not the same during grid faults.

This function can be included in the model by adding (a) a reference power calculation, (b) a selector that decides whether to output the p_{el} or the calculated reference power p_{mech} as mechanical output and (c) a decision logic. The logic could be based on two criteria, it is set if the voltage drops below a defined limit and is reset when p_{el} is close to p_{mech} again following voltage recovery.

D. Resulting generator model

The resulting generator model including current limitation, transformer and DC-link energy absorber is shown in Fig. 17.

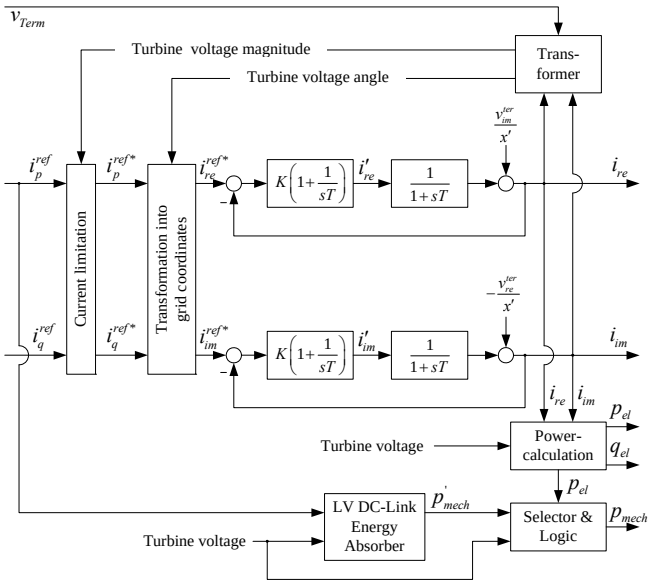

Fig. 17. Detailed Block diagram of aggregated generator model for DFIG and FSC

V. Validation Results

A. Measurement setup

According to [6] and [7], FRT – tests should be performed using the measurement setup described in Fig. 18. A PGU is connected to the grid through a testing device. The testing device is designed to reduce the voltage at the PGU to a specified level within a very short period of time. During normal operation, switch S1 is closed and switch S2 is open. In order to reduce the impact of activating impedance Z2 on the grid, in a first step switch S1 is opened. This connects a serial impedance Z1 in line with the PGU. After the transients have decayed, switch S2 is closed and the short circuit impedance Z2 is connected in parallel to the PGU. This causes a voltage dip at the PGU. After 150ms..2000 ms depending on the tests required, switch S2 is opened again. The voltage at the PGU then recovers. A short time later, switch S1 is closed, and normal operation is resumed.

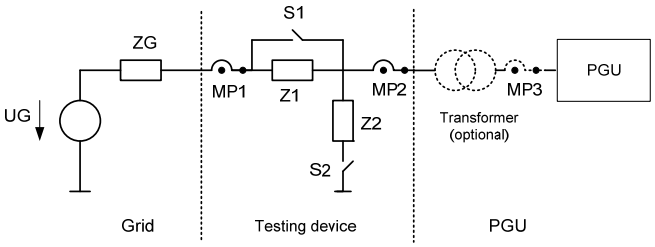

Fig. 18. Setup to measure the effect of voltage dips on a power generation unit, for example a wind turbine.

B. Measurements and Simulations

A simulation equivalent for a RMS measurement still has an “instantaneous” behavior, that means it also contains higher frequency components, even if positive and negative sequence are modeled separately. As a result, a 50 Hz filtering of the simulated values is necessary in order to have an equivalent to positive and negative sequence values of measurements. [6]. The turbine simulation model is based on the generic WECC/IEEE type 3 model [1], with a modified aerodynamic model according to [12] and the proposed generator model.

A voltage dip down to 20% rated voltage of a DFIG is shown in Fig. 19 for a 2 MW wind turbine. The reactive current reaches 1 pu during the fault in both measurement and simulation as required by German Grid codes.

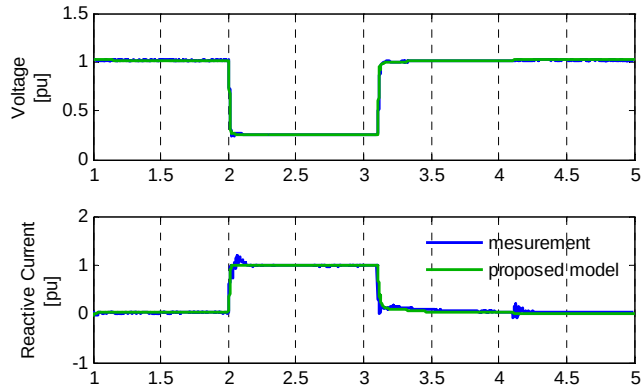

Fig. 19. Measurement and simulation of voltage and reactive current during voltage dip down to 20% rated voltage for wind turbine with DFIG operating at rated power

The simulation of the reactive current does not exactly reproduce the dynamics directly following the voltage reduction, but there is only a small error. During voltage recovery the reactive current contribution of measurement and

simulation are almost identical. The small oscillation of the measured current at t=4.2 seconds is due to the closing of switch S1 (see Fig. 18) and the resulting change of the voltage phase angle.

A comparable measurement for a FSC is shown in Fig. 20. There are only minor differences between measurement and simulation both during the grid fault and after the voltage recovery.

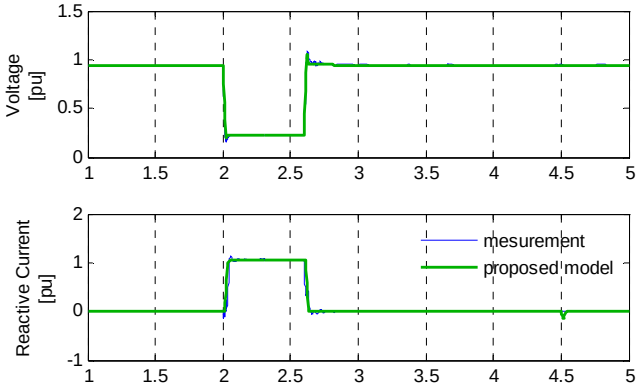

Fig. 20. Measurement and simulation of voltage and reactive current during voltage dip down to 20% rated voltage for wind turbine with FSC operating at rated power

A comparison of measurement and simulation of active power and active current of a DFIG during a voltage dip is shown in Fig. 21. Again the simplified model does not show all the dynamics of the measurement at the beginning of the fault, but as it can be seen, the average of simulation and measurement during the first 100ms following the grid are quite close to each other as required by [6].

The effect of the dynamic current limiter can be well observed during voltage recovery at t=3.2 seconds. Due to a phase angle shift and control actions of the inverter, the active current is reduced directly following the voltage recovery and then increased again with a given ramp rate limi-

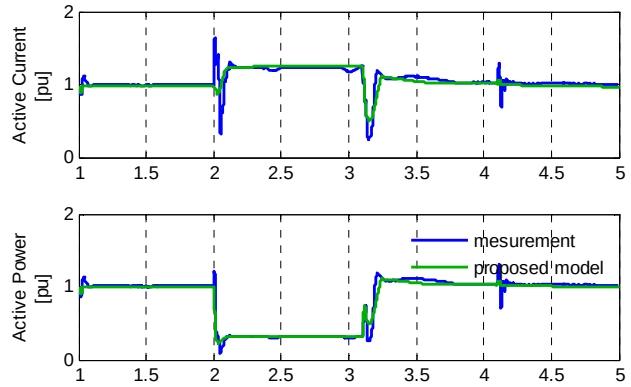

Fig. 21. Measurement and simulation of active current and active power during voltage dip down to 20% rated voltage for wind turbine with DFIG operating at rated power

tation. Although not the entire dynamics are reproduced, again a comparison of active power of measurement and simulation shows a good correlation.

As it can be seen in diagram 2 of Fig. 21, the active power recovery of the simulation starts slightly earlier and is slightly slower than in measurement. But as a result, the average of active power of both measurement and simulation during voltage recovery are close to each other. The average of the power correlates to the energy transferred, which is relevant because of its impact on the grid frequency. If the averages of both measurement and simulation are comparable, this means that the model provides a good representation of the impact of grid faults on frequency deviations in system studies.

Active current and active power of a FSC during a grid fault are shown in Fig. 22. Measurement and simulation show a very good correlation, although not all of the dynamics of the measurement are represented by the model. A different control strategy is used for the active current compared to Fig 21. The active current has now been reduced during the fault and active power recovery is not linear.

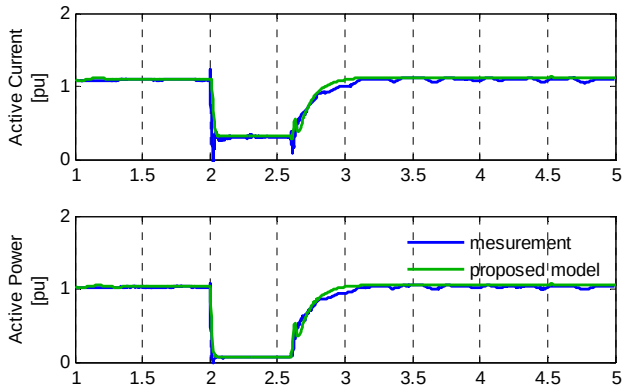

Fig. 22. Measurement and simulation of active current and active power during voltage dip down to 20% rated voltage for wind turbine with FSC operating at rated power

C. Validation results

Even though the comparison of Fig. 21 and Fig. 22 shows considerable differences in the control strategy of active power during grid faults, both approaches can be reproduced with the proposed model. The differences in control strategy do not depend on the technology chosen (DFIG or FSC) but on hardware design, control philosophy and grid code requirements.

The requirement for a generic model is to represent different approaches with an acceptable accuracy while keeping a simple modeling approach. The proposed model offers the possibility to configure the model response depending on the actual (manufacturer specific) implementation while still using a very limited number of parameters and a simple model structure.

VI. Summary

A simplified generic model for generator and inverter of both modern DFIG and FSC based wind turbines has been presented. The model is based on the existing generic WECC/IEEE type 3 and type 4 models, but allows an improved modeling of active and reactive currents during grid faults and during voltage recovery following grid faults.

The results of field test measurements of DFIG and FSC based wind turbines was compared to simulations using the proposed model and a very good correlation could be shown. The model will be proposed as extension to the existing WECC/IEEE generic models.

VII. References

[1] Generic Type-3 Wind Turbine-Generator Model for Grid Studies, WECC Wind Generator Modeling Group, Version 1.1, Sept. 14, 2006

[2] Price, W., Sanchez-Gasca, J.: "Simplified wind turbine generator aerodynamic models for transient stability studies" Power Systems Conference and Exposition, 2006. PSCE '06. 2006 IEEE PES, Oct. 2006.

[3] E.ON Netz GmbH, "Grid Code High and Extra high voltage", online: http://www.eon-netz.com/, Bayreuth, 2006

[4] Verordnung zu Systemdienstleistungen durch Windenergieanlagen (Systemdienstleistungsverordnung – SDLWindV), BMU, Germany-27.05.2009

[5] REE – Requisitos de respuesta frente a huecos de tension de las instalaciones de produccion de regimen especial, PO 12.3, November 2005;

[6] FGW: Technical Guidelines for Power Generating Units. Part 4 Demands on Modeling and Validating Simulation Models of the Electrical Characteristics of Power generation Units and Systems. Revision 4, September 15th, 2009

[7] FGW: Technische Richtlinien für Erzeugungseinheiten Teil 8 Zertifizierung der Elektrischen Eigenschaften von Erzeugungseinheiten und -anlagen am Mittel- Hoch- und Höchstspannungsnetz, Revision 1, 15. September 2009

[8] Procedure for Verification Validation and Certification of the Requirements of the PO 12.3 on the response of wind farm in the event of voltage dips, AEE, online: http://www.aeeolica.es/doc/privado/pvvc_v3_english.pdf

[9] Engelhardt, S., Feltes, C.; Fortmann, J.; Kretschmann, J.; Erlich, I.;: "Reduced Order Model of Wind Turbines based on Doubly-Fed Induction Generators during Voltage Imbalances", 8th International Workshop on Large-Scale Integration of Wind Power into Power Systems as well as on Transmission Networks for Offshore Wind Farms, Bremen 2009

[10] Erlich,I.; Kretschmann, J.; Fortmann, J.; et al., "Modeling of Wind Turbines based on Doubly-Fed Induction Generators for Power System Stability Studies", Modeling of Wind Turbines Based on Doubly-Fed Induction Generators for Power System Stability Studies, IEEE Transactions on Power Systems, Volume 22, Issue 3, Aug. 2007 Page(s):909 – 919

[11] Erlich, I.; Shewarega, C.; Engelhardt, S.; Kretschmann, J.; Fortmann, J.; Koch, F.; "Effect of Wind Turbine Output Current during Faults on Grid Voltage and the Transient Stability of Wind Parks" , IEEE Power and Energy Society General Meeting, Calgary, 2009

[12] Fortmann, J. "Generic Aerodynamic Model for Simulation of variable speed Wind Turbines", 9th International Workshop on Large-Scale Integration of Wind Power into Power Systems as well as on Transmission Networks for Offshore Wind Farms, Quebec City, 2010

VIII. Biographies

Jens Fortmann (1966) received his Dipl.-Ing. degree in electrical engineering from the Technical University Berlin, Germany, in 1996. From 1995 to 2002 he worked on the simulation of the electrical system and the control design of variable speed wind turbines at the different wind turbine manufacturers. Since 2002 he is with REpower Systems AG, Germany presently as team leader of model and system development He is the head of the FGW working group that specifies the modeling and model validation guideline TR4

Stephan Engelhardt (1967) received his Dipl.-Ing. degree in electrical engineering from the University Hannover, Germany, in 1997. Since 1997 he is with Woodward SEG GmbH & Co. KG, Kempen/Germany, presently head of the group Converter Technology and responsible for system designs and simulations, control strategies and patents.

Christian Feltes (1979) received his Dipl.-Ing. degree in electrical engineering from University of Duisburg-Essen/Germany in 2005. Since January 2006 he is doing his Ph.D. studies in the Department of Electrical Power Systems at the same University.
His research interests are focused on wind energy generation, control, integration and dynamic interaction with electrical grid.

Jörg Kretschmann (1958) received his Dipl.-Ing. degree in electrical engineering from the Technical University Berlin, Germany, in 1986. From 1986 to 1988 he worked for engineering department of AEG-Kanis in Essen, manufacturing of synchronous generators up to 200 MVA. Since 1988 he is with Woodward SEG GmbH & Co. KG, Kempen/Germany, as a designing engineer for speed-variable applications: uninterruptible power supply, shaft alternators, DFIG for wind turbines.

Martin Janßen (1970) studied electrical engineering at Ruhr-University Bochum, Bochum, Germany, and Purdue University, West Lafayette, IN, from 1990 to 1995, and received the Dr. Ing. degree from Ruhr-University in 2000. From 1995 to 2000, he was a Researcher with the Chair for Generation and Application of Electric Energy, Ruhr-University Bochum. Since 2001 he is with Converteam GmbH, Berlin, Germany working in the area of control of high-power converters.

Tobias Neumann (1977) received his Dipl.-Ing. degree in electrical engineering from the University of Duisburg-Essen/Germany in 2009. Since January 2010 he is doing his Ph.D. studies in the Department of Electrical Power Systems at the same University.

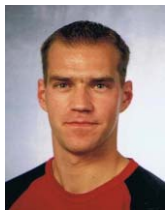

His research interests include wind power generation, mainly focussing on control and modelling as well as DSP programming.

Istvan Erlich (1953) received his Dipl.-Ing. degree in electrical engineering from the University of Dresden/Germany in 1976. After his studies, he worked in Hungary in the field of electrical distribution networks. From 1979 to 1991, he joined the Department of Electrical Power Systems of the University of Dresden again, where he received his PhD degree in 1983. In the period of 1991 to 1998, he worked with the consulting company EAB in Berlin and the Fraunhofer Institute IITB Dresden. Since 1998, he is Professor and head of the Institute of Electrical Power Systems at the University of Duisburg-Essen/Germany. His major scientific interest is focused on power system stability and control, and modeling of power system dynamics including intelligent system applications.